Original Article

MiR-495-3p depletion contributes to myocardial ischemia/reperfusion injury in cardiomyocytes by targeting TNC

Wei Song [a], Naiyan Qiu [b], *

[a] Department of Cardiology, Taizhou Central Hospital (Taizhou University Hospital), 999 Donghai Avenue, Jiaojiang District, Taizhou, Zhejiang Province, China
[b] Department of Cardiology, The Fifth People's Hospital of Jinan, No. 24297 Jingshi Road, Huaiyin District, Jinan, Shandong Province, 250021, China

ABSTRACT

Background: Tenascin-C (TNC) has been found to abnormally express in myocardial ischemia/reperfusion injury (MI/RI), but its effect on cardiomyocytes apoptosis is unknown and is worthy of investigation.
Methods: H9C2 cells were given hypoxia/reoxygenation (H/R) treatment to obtain the replica of MI/RI in vitro. The effect of H/R on viability, apoptosis and inflammation was studied by CCK-8 assay, flow cytometry, mitochondrial membrane potential (MMP) and Ca^{2+} measurements as well as enzyme linked immunosorbent assay. We applied bioinformatics analysis and luciferase reporter assay to screened and validated TNC-targeting miR-495-3p which was then mechanistically investigated by quantitative real-time polymerase chain reaction (qRT-PCR) and Western blot. With the assistance of cell transfection, rescue assays were conducted.
Results: H9C2 cells showed diminished viability, accelerated apoptosis, elevated tumour necrosis factor alpha (TNF-α) and interleukin 1 beta (IL-1β), and TNC overexpression in response to H/R induction, while silencing of TNC partially reversed the effect of H/R treatment on the H9C2 cells. TNC silencing reduced Ca^{2+} level and enhanced MMP level in the H/R-stimulated cells. MiR-495-3p targeted TNC and showed a low expression in the H/R-stimulated cells. The expression of TNC was negatively regulated by miR-495-3p. Inhibition of miR-495-3p repressed viability and MMP level, and facilitated apoptosis and levels of Ca^{2+}, TNF-α and IL-1β in the H/R-stimulated cells. The effect of TNC silencing and miR-495-3p depletion on H/R-induced cardiomyocyte injury was mutually reversed in vitro.
Conclusion: MiR-495-3p targeted TNC to regulate the apoptosis and inflammation of cardiomyocytes in H/R induction, which was associated with Ca^{2+} overload.
© 2022, The Japanese Society for Regenerative Medicine. Production and hosting by Elsevier B.V. This is an open access article under the CC BY-NC-ND license (http://creativecommons.org/licenses/by-nc-nd/4.0/).

1. Introduction

Myocardial infarction has become one of the most common causes of death worldwide amid an ageing population and changes in people's diets, posing a serious threat to human physical and mental health [1]. Acute myocardial infarction (AMI) is a type of heart disease mostly as a result of sudden occlusion of the epicardial coronary arteries which causes ischemia and hypoxia in the myocardium [2]. At present, myocardial injury due to ischemia-reperfusion may account for nearly 50% cases of the eventual myocardial injury in AMI [3]. A timely opening of the infarct-related vessels and restoration of myocardial perfusion are currently the most effective treatments for this condition [3]. However, the ischemic myocardium is then re-perfused with blood, resulting in additional injury, namely myocardial ischemia/reperfusion injury (MI/RI), such as increased apoptosis, arrhythmias, impaired myocardial energy metabolism and abnormal hemodynamics, which exacerbates the damage to myocardial tissues [4]. Therefore, how to prevent or mitigate MI/RI is one of the current hot issues in the field of cardiovascular disease research.

Tenascin-C (TNC) is an extracellular matrix glycoprotein that is ephemerally expressed during embryogenesis, and only at a very low level in mature organs, unless the expression of TNC is upregulated under specific pathological conditions such as inflammation, infection, tumor, injury and remodeling [5–7]. TNC have a significant association with the severity of atherosclerosis, and TNC level significantly increased as the risk of coronary artery disease

* Corresponding author. Department of Cardiology, The Fifth People's Hospital of Jinan, No. 24297 Jingshi Road, Huaiyin District, Jinan City, Shandong Province, 250021, China.
E-mail address: qiuunaiya_qny@163.com (N. Qiu).

Peer review under responsibility of the Japanese Society for Regenerative Medicine.

increased [8]. When the heart is attacked by a variety of cardiac diseases or cardiac injury, the TNC expression will be triggered and re-expressed [9,10]. TNC expression has been linked to an exaggerated repair process after myocardial infarction with reduced interstitial fibrosis reported in TnC-deficient mice following coronary artery ligation [11]. In addition, TNC inhibits cardiac endothelial cell spreading and enhances migration in response to angiogenic growth factors [12]. It has been found that TNC was identified as a gene that is abnormally expressed in MI/RI [13,14]. In addition, Jin et al. found a correlation between TNC and early atherosclerosis and vascular injury in a mouse model [15]. But, the specific mechanism of TNC in the development of MI/RI is poorly understood.

MicroRNAs (miRNAs) are a class of post-transcriptional regulators that negatively regulate the translation of genes by specifically binding to their target mRNA [16]. In recent years, extensive studies have confirmed that miRNAs play a very important regulatory role in cardiovascular diseases such as myocardial injury, arrhythmias and vascular lesions [17]. Moreover, a number of miRNAs have now been currently found to be involved in the process of MI/RI [18–20]. MiR-495-3p is a member of the miRNA family, which is closely associated with cell apoptosis and inflammatory responses [21,22]. A new study reports that the inhibition of miR-495-3p expression promotes apoptosis of cardiomyocytes [23].

Through the analysis of data set GSE160516, we found that MI/RI treatment would cause differences in gene expression in mice, and found that TNC was identified as the gene with abnormal expression of MI/RI, but the specific mechanism remains unclear. Therefore, we probed into the function of TNC and the interaction of TNC and miR-495-3p in the apoptosis of cardiomyocytes undergone MI/RI. As identified in this study, the miR-495-3p/TNC axis is an important contributor to the damage that occurs in cardiomyocytes during MI/RI, which provides a theoretical basis for improving in the clinical treatment of ischemic heart disease and facilitating the prognosis of patients with AMI.

2. Material and methods

2.1. Cell grouping and treatment

H9C2 cell line (CRL-1446; American Type Culture Collection, Manassas, VA, USA) derived from rat heart tissues was used as the subject in this research. The cells were subject to grow in a culture medium (DMEM, 30-2002, American Type Culture Collection, Manassas, VA, USA) supplementing 10% fetal bovine serum (FBS, abs973, Absin, Shanghai, China) in an incubator (37 °C, 5% CO_2). After subculturing, the cardiomyocytes were harvested and seeded into 6-well plate (2×10^5 cells/well) and then divided into groups
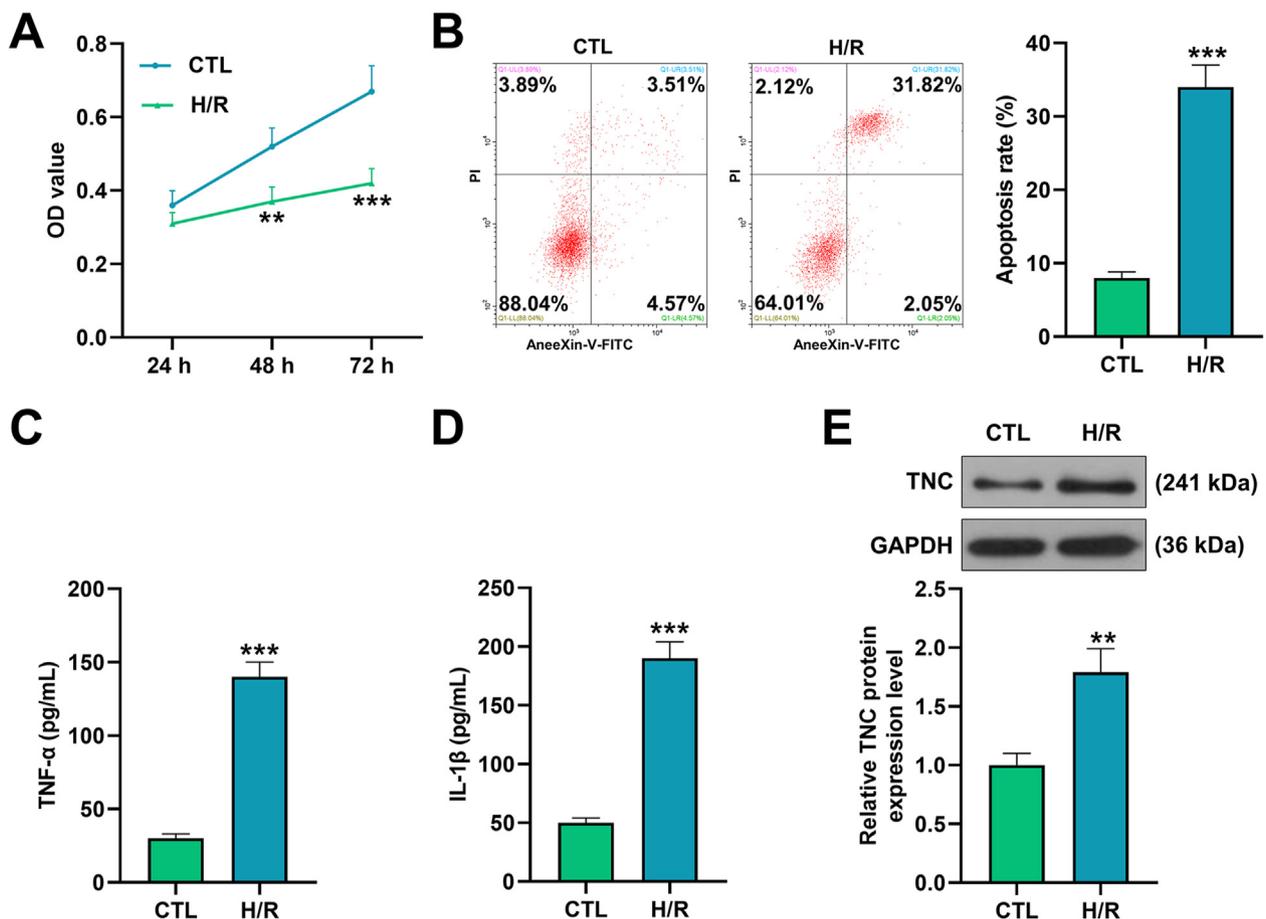
Fig. 1. The effect of H/R induction on viability, apoptosis and TNC expression in H9C2 cells. (A) CCK-8 assay was used to measure OD value in H9C2 cells after H/R treatment. (B) Then, flow cytometry was applied to analyze apoptotic cells. (C) ELISA was employed to determine the level of inflammatory cytokines (TNF-α, IL-1β). (E) Western blot was performed to detect TNC protein level in H/R-induced H9C2 cells. GAPDH served as an internal reference. **$p < 0.01$, ***$p < 0.001$ vs. CTL. CCK-8, cell counting kit-8; OD, optical density; TNC, tenascin-C; ELISA, enzyme linked immunosorbent assay; TNF-α, tumour necrosis factor alpha; IL-1β, interleukin 1 beta; GAPDH, glyceraldehyde-3-phosphate dehydrogenase; H/R, hypoxia/reoxygenation.
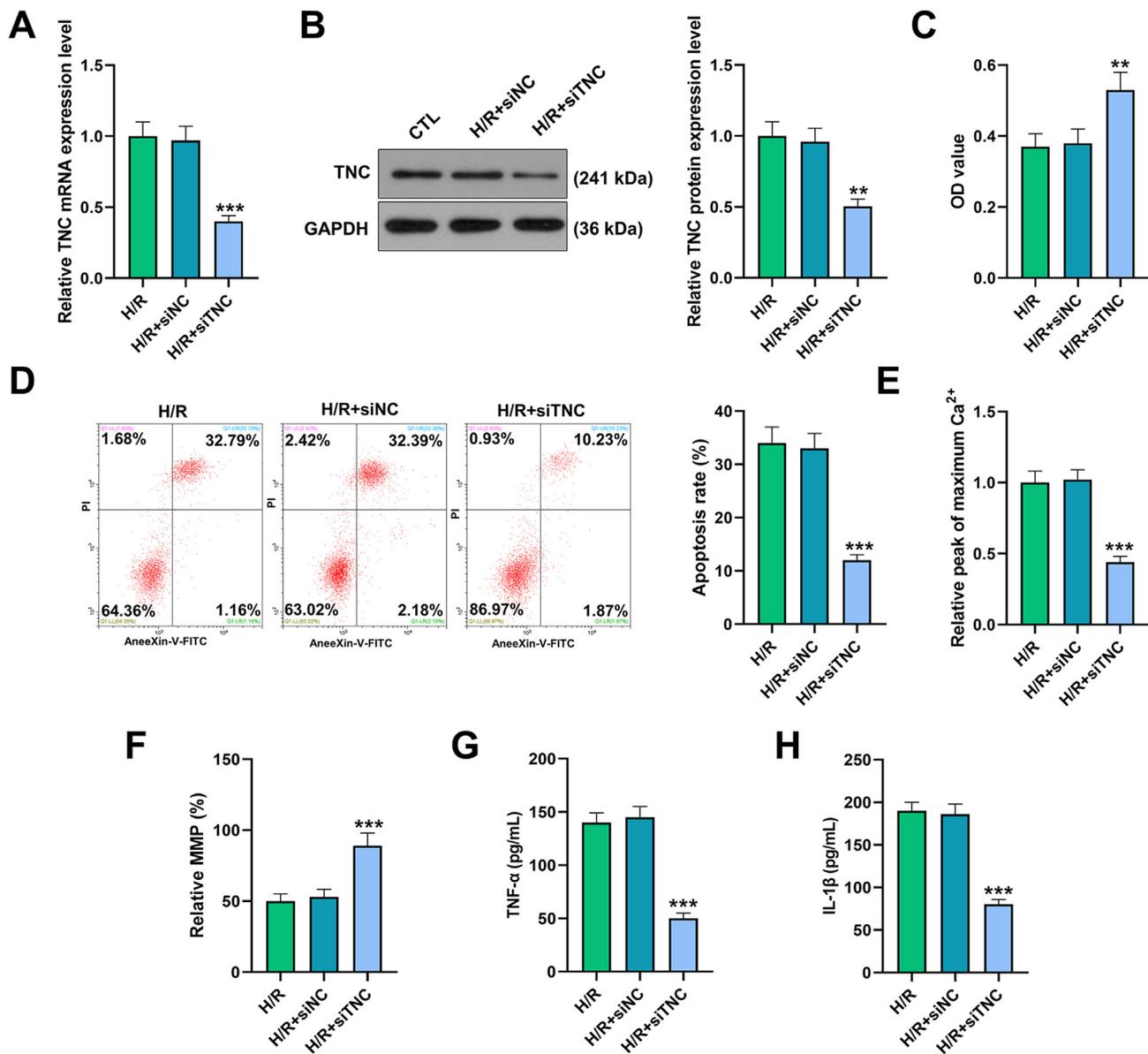
Fig. 2. The effect of TNC silencing on viability, apoptosis and MMP of H9C2 cells after H/R treatment. (A) After siTNC transfection, qRT-PCR was performed to detect TNC expression in H/R-induced cells. GAPDH served as an internal reference. (B) Next, the protein level of TNC was determined by Western blot. GAPDH served as an internal reference. (C) CCK-8 assay was used to measure the viability of H9C2 cells with TNC silencing after H/R induction. (D) The cell apoptosis was then detected by flow cytometry. (E) The content of Ca^{2+} in H9C2 cells was determined by colorimetry after H/R induction or/and TNC inhibition. (F) MMP level in H9C2 cells after TNC inhibition or/and H/R stimulation was measured by JC-1 MMP assay kit. (G-H) ELISA was employed to determine the level of inflammatory cytokines (TNF-α, IL-1β) in H9C2 cells undergone H/R induction or/and TNC inhibition. **$p < 0.01$, ***$p < 0.001$ vs. H/R + siNC. CCK-8, cell counting kit-8; qRT-PCR, quantitative real-time polymerase chain reaction; TNC, tenascin-C; GAPDH, glyceraldehyde-3-phosphate dehydrogenase; ELISA, enzyme linked immunosorbent assay; TNF-α, tumour necrosis factor alpha; IL-1β, interleukin 1 beta; MMP, mitochondrial membrane potential; H/R, hypoxia/reoxygenation; si, small interfering; NC, negative control.

of control (CTL), hypoxia/reoxygenation (H/R), H/R + small interfering RNA against TNC (siTNC), H/R + siRNA negative control (siNC), H/R + miR-495-3p inhibitor (I) + siTNC, H/R + I + siNC, H/R + inhibitor control (IC) + siTNC and H/R + IC + siNC. The medium-cultured cells in H/R groups were stimulated with 95% N_2 and 5% CO_2 in a humidified chamber for 6 h (h), followed by exposure to room air 5% CO_2 and 95% O_2 for another 6 h, according to the previous descriptions [24]. After that, the induced cells were re-suspended and collected for cell counting kit-8 (CCK-8) assay.

2.2. Cell transfection

Subcultured H9C2 cells (2×10^5 cells/well) were required to incubate into a 6-well plate overnight. Next, siTNC (5′-

GGUUGGUUACUUCAAUCAAUG-3′), miR-495-3p I (5′-AAGAA-GUGCACCAUGUUUGUUU-3′, 100 nM, GenePharma, Shanghai, China), siNC and IC were used to transfect the specified cells by Lipofectamine 3000 (L3000015, Invitrogen, Carlsbad, CA, USA) ahead of cell treatment. Thereafter, quantitative real-time polymerase chain reaction (qRT-PCR) was carried out for TNC or miR-495-3p expression verification.

2.3. Bioinformatics analysis and luciferase reporter assay

MiRNAs possibly targeting TNC were predicted by three databases of miRDB (http://mirdb.org/miRDB/index.html), Targetscan (http://www.targetscan.org/vert_71/) and microT (http://www.microrna.gr/microT), and all data were illustrated in the form of a
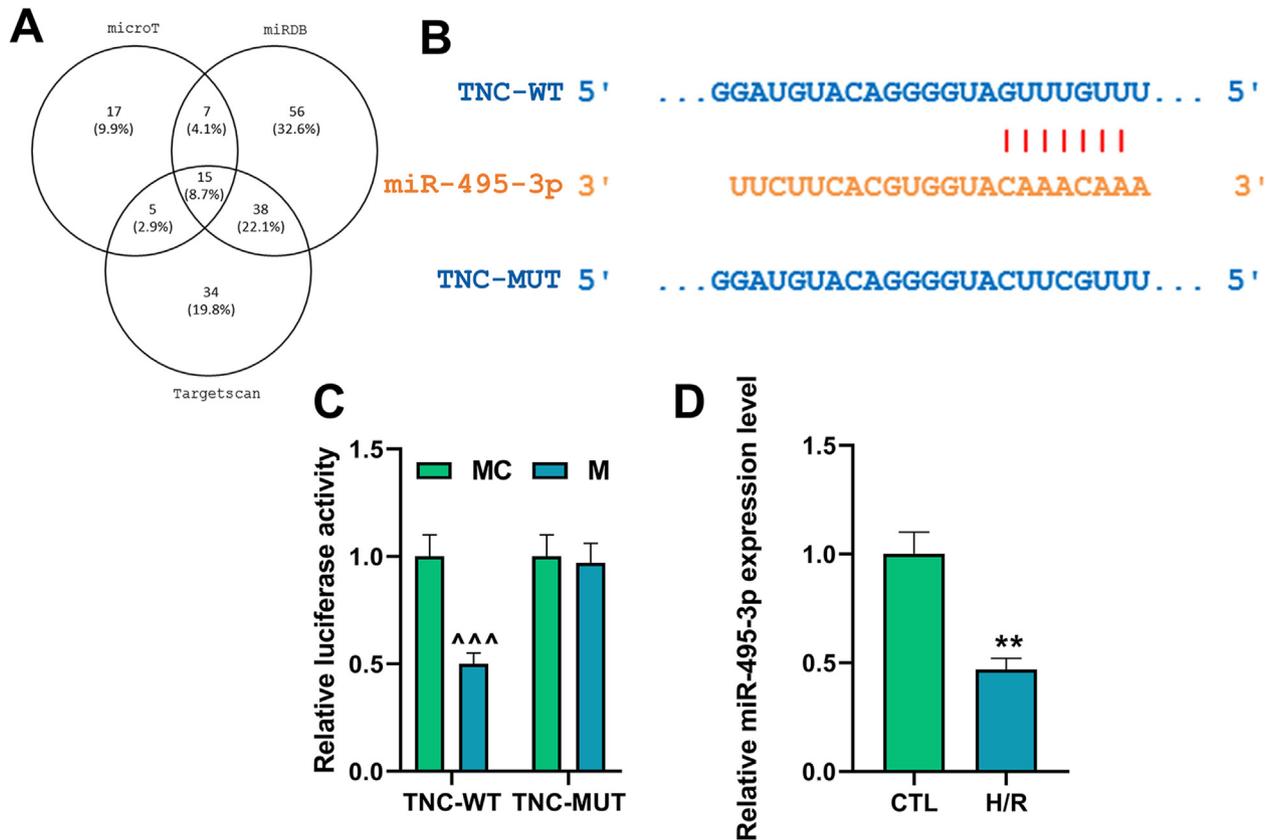
Fig. 3. MiR-495-3p targeted TNC in H9C2 cells. (A) Candidate miRNAs targeting TNC were screened out by miRDB (http://mirdb.org/miRDB/index.html), Targetscan (http://www.targetscan.org/vert_71/) and microT (http://www.microrna.gr/microT). (B) The binding sites between miR-495-3p and TNC were predicted by Starbase. (C) Dual luciferase reporter assay was employed to investigate the interaction between miR-495-3p and TNC. (D) The expression of miR-495-3p in H9C2 cells after H/R induction was determined by qRT-PCR. U6 served as an internal reference. $**p < 0.01$ vs. CTL; $^{^^^}p < 0.001$ vs. MC. qRT-PCR, quantitative real-time polymerase chain reaction; TNC, tenascin-C; H/R, hypoxia/reoxygenation; CTL, control; MC, mimic control; M, miR-495-3p mimic; WT, wild-type; MUT, mutant-type.

Venn diagram. After literature comparisons, we selected miR-495-3p among 15 screened candidate miRNAs to be used for follow-up studies.

Given the binding sites predicted by Starbase, we then conducted luciferase reporter assay to validate this target relationship. We used Vectors (E1330, Promega, Madison, WI, USA) to create wild-type of TNC (TNC-WT, 5′-GGAUGUACAGGGGUAGUUUGUUU-3′) and mutant-type of TNC (TNC-MUT, 5′-GGAUGUACAGGGGUA-CUUCGUUU-3′) which were then independently co-transfected with miR-495-3p mimic (M) and miR-495-3p mimic control (MC) into H9C2 cells (5×10^4 cells/well, 24-well plates) using Lipofectamine 3000. Afterwards, relative luciferase activity was measured by Dual-Luciferase Reporter Assay System (E1910, Promega, USA) according to the technical manual.

2.4. Western blot

The total protein of H9C2 cells were lysed using RIPA Buffer (AR0105) and measured the concentration of lysate by BCA Protein Assay Kit (AR1189A). The protein sample was separated by sodium dodecyl sulfate polyacrylamide gel electrophoresis and transferred onto the PVDF membranes (AR0136-02) which were subsequently submerged in Blocking Buffer (AR0174) for 1 h at room temperature, and then were incubated with primary antibodies of TNC (ab108930, 1/1000, 241 kDa, Abcam, Cambridge, UK) and Glyceraldehyde-3-phosphate dehydrogenase (GAPDH, ab9484, 1/10000, Abcam, UK) at 4 °C overnight. Afterwards, the membranes were incubated with Goat Anti-Rabbit IgG (ab205718, 1/2000, Abcam,

UK) and Goat Anti-Mouse IgG (ab205719, 1/2000, Abcam, UK) at room temperature for 2 h iBright Imaging System (CL750, Invitrogen, USA) and ECL Substrates (AR1191) were used to develop protein bands. GAPDH served as the internal control. All reagent products used were supplied by Boster Biological Technology (China).

2.5. RNA isolation and qRT-PCR

H9C2 cells undergone different treatments were isolated total RNA with Extraction Reagent (RE001, Synthgene, Nanjing, China). The extract was treated with SuperScript One-Cycle cDNA Kit (A10752030, ThermoFisher, Waltham, MA, USA) to synthesize cDNAs. QRT-PCR was subsequently conducted using YBR Premix Ex Taq II (RR820A, Takara, Tokyo, Japan) in the Real-Time PCR System (MX3000P, Stratagene, Santa Clara, CA, USA). The mRNA levels for TNC and miR-495-3p were calculated by $2^{-\Delta\Delta Ct}$ method [25], with GAPDH or U6 using for normalization. All primers employed for amplification as follows:

TNC, forward: 5′-TTTGCCCTCACTCCCGAAG-3'; reverse: 5′-AGGGTCATGTTTAGCCCACTC-3′
GAPDH, forward: 5′-CTCCTCCACCTTTGACGCTG-3'; reverse: 5′-TCCTCTTGTGCTCTTGCTGG-3′
miR-495-3p, forward: 5′-GCGAAACAAACATGGTGC-3'; reverse: 5′-GCAGGGTCCGAGGTATTC-3′
U6, forward: 5′-CTCGCTTCGGCAGCACA-3'; reverse: 5′-AACGCTTCACGAATTTGCGT-3′
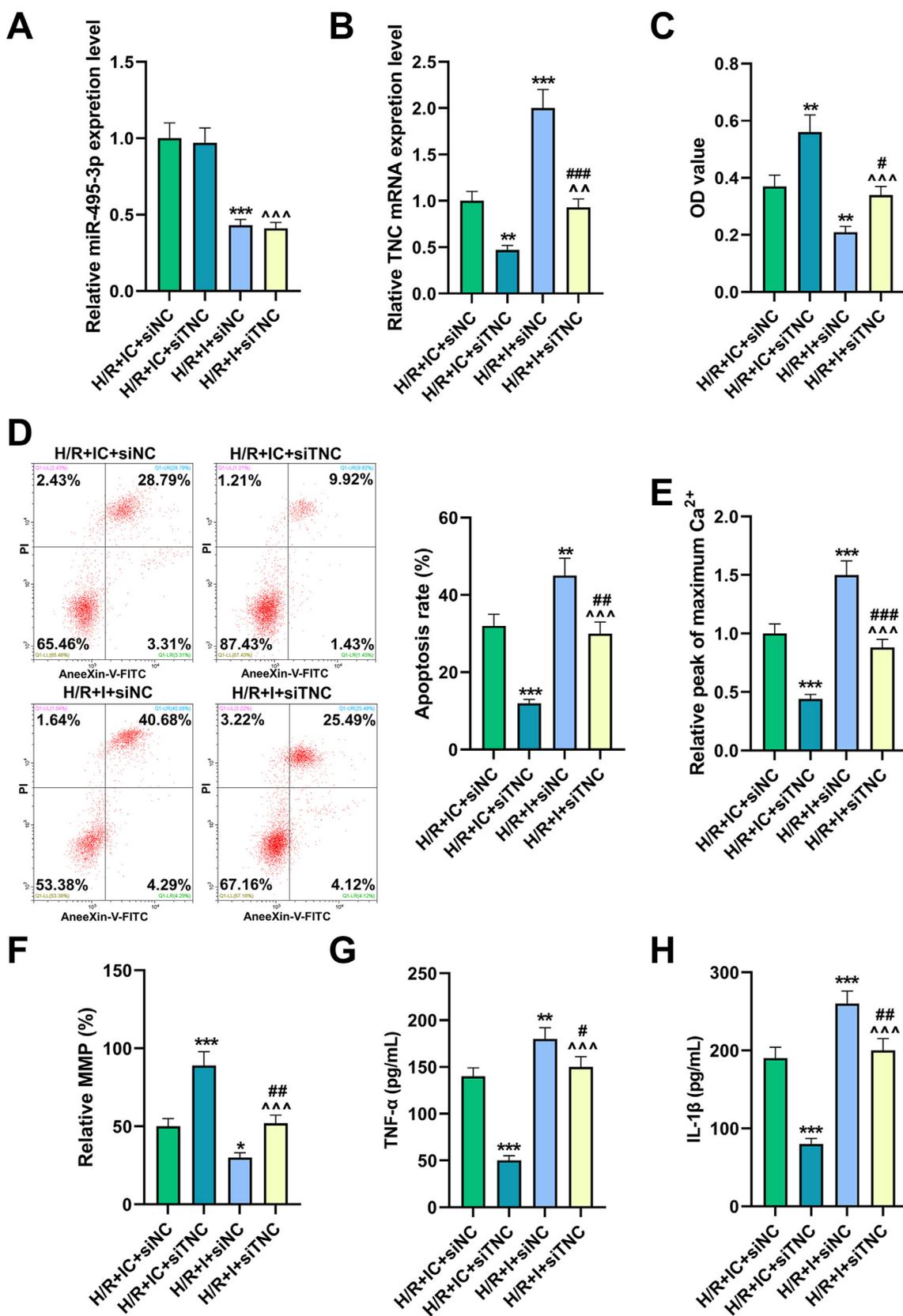
2.6. CCK-8 assay

After H/R induction, the cell viability of H9C2 cells was determined using CCK-8 Kit (96992, Sigma-Aldrich, St. Louis, MO, USA). 100 μl cell suspension was added into a 96-well plate (1×10^4 cells/well) and incubated for 24, 48 or 72 h, and then 10 μl CCK-8 solution was added and co-incubated for 2 h at 37 °C of 5% CO_2. The optical density (OD) value was detected at 450 nm using a microplate reader (MR-96A, Mindary, Shenzhen, China).

2.7. Flow cytometry

After 48 h of H/R-induction treatment, we applied Annexin V-FITC/PI Apoptosis Detection Kit (E-CK-A211, Elabscience, Wuhan, China) to stain H9C2 cells before apoptosis determination. First, the cells were required to adjust the density to 1×10^5 cells/ml. After centrifugation and re-suspension, 5 μl Annexin V-FITC and 5 μl PI were subjected to stain the cells for 15 min (min) in the dark. Lastly, the stained cells were run on a flow cytometer (Attune NxT, ThermoFisher, USA) for detecting apoptotic H9C2 cells.

2.8. Measurement of Ca^{2+} concentration

Following interference with TNC or/and miR-495-3p, the concentration of Ca^{2+} in H/R-induced H9C2 cells were measured with the employment of Calcium Colorimetric Assay Kit (S1063S, Beyotime, Shanghai, China). In brief, Sample Lysis Buffer was used to mixed with the cells thoroughly in a 6-well plate, and the lysate was collected after a 5-min centrifugation at 10,000 rpm. Then, 150 μl o-cresolphthalein complexone solution was prepared and added into each well at room temperature, followed by a 10-min incubation. After reading absorbance at 575 nm by the MR-96A reader, Ca^{2+} concentration was calculated according to the protocol.

2.9. Mitochondrial membrane potential (MMP) assay

MMP changes in H/R, H/R + siNC, H/R + siTNC, H/R + IC + siNC, H/R + IC + siTNC, H/R + I + siNC and H/R + I + siTNC after 48 h were determined by MMP Kit (with JC-1) (E-CK-A301, Elabscience, China). Briefly, the induced cells (1×10^5 cells/ml) were washed with Phosphate-Buffered Saline (PBS, C0221A, Beyotime, China) and re-suspended after centrifugation. 500 μl JC-1 staining solution was used to treat the cells for 15 min at 37 °C. After that, the stained cells were performed centrifugation and rinsed with precooled $1 \times$ JC-1 Assay Buffer twice. Lastly, the flow cytometer was applied for detection within 30 min.

2.10. Enzyme linked immunosorbent assay (ELISA)

Levels of tumour necrosis factor alpha (TNF-α) and interleukin 1 beta (IL-1β) in H9C2 cells undergone H/R induction or/and cell transfection were determined using Rat ELISA Kit (ER1393, ER1094,

FineTest, Wuhan, China). Briefly, the collected cells were diluted with Sample Dilution Buffer and incubated in the ELISA microplate at 37 °C for 90 min, followed by adding Biotin-labeled Antibody. After 1 h, the cells in each well were treated with 100 μl HRP-Streptavidin Conjugate for 30 min and 90 μl TMB Substrate for 20 min, in sequence. The absorbance at 450 nm was read using the MR-96A reader immediately when the cells were added with Stop Solution.

2.11. Statistical analysis

Measurement data was demonstrated as the mean ± standard deviation and analyzed with Software GraphPad Prism 8.0 (GraphPad Software, USA). Independent samples *t*-test was used to compare the differences between two groups. One-way analysis of variance was applied for the comparison of multiple groups. $P < 0.05$ was defined as a statistically significance.

3. Results

3.1. H/R treatment inhibited the viability but promoted the apoptosis, inflammation and TNC expression of cardiomyocytes

As shown in Fig. 1A, the OD value was decreased at 48 h and 72 h of H/R-induced H9C2 cells, compared to CTL group ($p < 0.01$). In view of the significantly inhibiting effect of H/R treatment on cell viability at 48 h, we selected 48 h as the induction time in the subsequent experiments. The apoptosis of H/R-induced H9C2 cells was significantly intensified compared with CTL group (Fig. 1B, $p < 0.001$). Besides, levels of TNF-α and IL-1β in the cells were considerably up-regulated after H/R treatment (Fig. 1C and D, $p < 0.001$). Moreover, Western blot measured that comparing to CTL group, TNC protein level was elevated in the cells treated with H/R (Fig. 1E, $p < 0.01$).

3.2. TNC silencing ameliorated the inflammation-mediated injury of cardiomyocytes induced by H/R

To figure out the role of TNC in MI/RI, we transfected siTNC into H9C2 cells followed by H/R treatment. The results of qRT-PCR identified that the mRNA level of TNC was strikingly suppressed in H/R + siTNC group compared to the group of H/R + siNC (Fig. 2A, $p < 0.001$). Consistently, the protein level of TNC which was determined by Western blot showed the same result (Fig. 2B, $p < 0.01$). Subsequently, CCK-8 assay detected that the viability of H9C2 cells in the H/R environment was robustly improved by siTNC (Fig. 2C, $p < 0.01$). In contrast, the cell apoptotic was decreased by siTNC, with H/R induction (Fig. 2D, $p < 0.001$). As shown in Fig. 2E, the peak level of Ca^{2+} was lower in the group of H/R + siTNC than that in the group of H/R + siNC ($p < 0.001$). Additionally, TNC silencing significantly increased MMP in H/R-induced cells (Fig. 2F, $p < 0.001$). Also, the enhanced levels of TNF-α and IL-1β by H/R treatment was reversed after down-regulating TNC in the cells (Fig. 2G and H, $p < 0.001$).

Fig. 4. MiR-495-3p played a regulatory effect on viability, apoptosis and MMP of H/R-induced H9C2 cells by targeting TNC. (A-B) The expressions of miR-495-3p and TNC in H/R-induced cells transfected with miR-495-3p inhibitor or siTNC or both of them were determined by qRT-PCR. U6 or GAPDH served as an internal reference. (C) Subsequently, CCK-8 assay was conducted to detect OD value for evaluating cell viability. (D) Also, the apoptosis of specified cells with H/R was assessed by flow cytometry. (E) The content of Ca^{2+} in H/R-induced H9C2 cells was determined by colorimetry after interference with TNC or/and miR-495-3p. (F) JC-1 MMP assay kit was used to measure MMP of H/R-induced cells interfered with TNC or/and miR-495-3p. (G-H) ELISA was employed to determine the level of inflammatory cytokines (TNF-α, IL-1β) in H/R-induced H9C2 cells after interference with TNC or/and miR-495-3p. *$p < 0.05$, **$p < 0.01$, ***$p < 0.001$ vs. H/R + IC + siNC; ¨$p < 0.01$, ¨¨$p < 0.001$ vs. H/R + IC + siTNC; #$p < 0.05$, ##$p < 0.01$, ###$p < 0.001$ vs. H/R + I + siNC. CCK-8, cell counting kit-8; OD, optical density; qRT-PCR, quantitative real-time polymerase chain reaction; TNC, tenascin-C; GAPDH, glyceraldehyde-3-phosphate dehydrogenase; ELISA, enzyme linked immunosorbent assay; TNF-α, tumour necrosis factor alpha; IL-1β, interleukin 1 beta; MMP, mitochondrial membrane potential; H/R, hypoxia/reoxygenation; si, small interfering; NC, negative control; IC, inhibitor control.

3.3. MiR-495-3p directly targeted TNC in cardiomyocytes

As illustrated in Fig. 3A, Venn diagram screened out 15 miRNAs that potentially targeted TNC in cardiomyocytes by overlapping the data resulted from miRDB, Targetscan and microT databases. After precisely investigation, we obtained the predicted binding sites between miR-495-3p and TNC by Starbase (Fig. 3B). The result of luciferase assay confirmed that TNC was targeted by miR-495-3p given that miR-495-3p overexpression visibly inhibited luciferase activity in the cells with TNC-WT (Fig. 3C, $p < 0.001$). Also, miR-495-3p expression was decreased in H/R-induced H9C2 cells (Fig. 3D, $p < 0.01$).

3.4. MiR-495-3p depletion blunted the protecting effect of TNC silencing on H/R-induced cardiomyocytes

To unveil the regulatory mechanism of miR-495-3p in MI/RI and its effect on TNC, we transfected miR-495-3p inhibitor or co-transfected miR-495-3p inhibitor and siTNC into H9C2 cells followed by H/R induction. As Fig. 4A presented, miR-495-3p inhibitor remarkably diminished miR-495-3p expression in the group of H/R + I + siNC, and also reduced miR-495-3p expression in the group of H/R + I + siTNC ($p < 0.001$). Interestingly, qRT-PCR detected that miR-495-3p inhibitor considerably up-regulated TNC expression in H9C2 cells treated with H/R in comparing to H/R + IC + siNC group, and the reduction of TNC expression caused by siTNC was partially reversed by additional transfection of miR-495-3p inhibitor (Fig. 4B, $p < 0.01$). According to the following rescue experiments, miR-495-3p depletion impaired viability (Fig. 4C, $p < 0.01$), accelerated apoptosis (Fig. 4D, $p < 0.01$), elevated the peak level of Ca^{2+} (Fig. 4E, $p < 0.001$), reduced the level of MMP (Fig. 4F, $p < 0.05$) and increased TNF-α and IL-1β levels (Fig. 4G and H, $p < 0.01$) in the cells undergone H/R treatment, which were all counteracted by TNC silencing (Fig. 4C–H, $p < 0.05$). Likewise, the promoting effect of TNC silencing on the viability and MMP level and the inhibiting effect of TNC silencing on the apoptosis and Ca^{2+}, TNF-α and IL-1β levels in the H/R-induced cells were reversed by miR-495-3p inhibitor (Fig. 4C– H, $p < 0.001$).

4. Discussion

MI/RI is a complicated pathological process that includes cell apoptosis, inflammatory response, impaired function of mitochondrial membranes, dysregulation of nitric oxide metabolism, endothelial cell dysfunction, and the generation of reactive oxygen species (ROS) [26]. Cell apoptosis, known as programmed cell death, occurs in many physiological or pathological processes which is regulated by a variety of genes and multi-level substances, and which plays a vital role in the healthy development of embryonic tissues and the maintenance of the steady state of organs [27]. Previously, it has been shown that apoptosis is a major destiny of cardiomyocytes undergone MI/RI, as well as is one of the main factors affecting the outcome of reperfusion in AMI [28,29]. In addition, animal experiments by Shiroto et al. proved that inhibition of cardiomyocyte apoptosis strikingly attenuated MI/RI [30]. In this study, we gave H9C2 cells H/R treatment to obtain the replica of MI/RI *in vitro*, and determined cell viability and apoptosis. As a result, H9C2 cells presented diminished viability and increased apoptosis in response to H/R induction. Previously, we found that 72 h ischemia-reperfusion treatment resulted in differential gene expression in mice through analysis of the dataset GSE160516. After selecting the top 5 genes for online search and analysis, TNC was found to be significantly aberrantly expressed in MI/RI [31]. Expectedly, we verified its overexpression in H/R-induced H9C2 cells in this study, moreover, silencing of TNC promoted the

viability and inhibited the apoptosis of H/R-treated H9C2 cells, it indicated that TNC silencing alleviates H/R induced myocardial cell injury.

After reperfusion of the ischemic myocardium, although the blood supply is restored, the increased production of ROS and the overload of calcium ions during ischemia inevitably lead a cascade of inflammatory responses in the cardiomyocytes, eventually triggering the apoptotic program [32]. MI/RI-induced inflammatory response has been confirmed to further exacerbate myocardial injury [33]. In the *in vitro* study of MI/RI, pro-inflammatory cytokines including IL-6, TNF-α and IL-1β were expressed at high levels in H/R-induced cardiomyocytes [34]. In myocardial injury, TNF-α has been found to contribute to cardiomyocyte injury by inducing infiltration of a huge number of neutrophils into the myocardium [35]. Additionally, IL-1β has been proven to function as a pivotal role in ROS accumulation in H/R-induced cardiomyocytes by activating arachidonic acid and recruiting neutrophils [36]. In this study, we found that both upregulations of TNF-α and IL-1β in H9C2 cells after H/R induction, and silencing of TNC inhibited level of TNF-α and IL-1β in H/R-treated H9C2 cells. Taken together, it is suggested that silencing of TNC inhibiting myocardial apoptosis and inflammation could be an effective strategy for the alleviation of MI/RI.

Recently, Tong et al. found that TNC thriving was responsible for neuronal apoptosis and inflammation after subarachnoid hemorrhage [37]. Later, TNC was reported to play a immunomodulatory role in the inflammation-driven cardiomyopathy [38]. Mitochondria play a role in cell apoptosis by regulating the release of cytochrome C and ROS [39]. During the MI/RI, mitochondria undergo ATP shortage and catabolism which causes an imbalance in MMP, thereby resulting in the opening of the mitochondrial permeability transition pore (mPTP) and the release of cytochrome C to activate apoptosis [40]. In the other hand, Ca^{2+} overload in cardiomyocytes caused by the dysfunction of mitochondria has been considered as one of classic onsets of MI/RI [41,42]. In our study, we found that TNC silencing not only significantly ameliorated apoptosis and enhanced viability and MMP of H9C2 cells after H/R induction but also reduced the level of Ca^{2+}, TNF-α and IL-1β, indicating that suppressing TNC could exert a protecting effect on MI/RI by repairing mitochondria to suppress apoptosis and inflammatory response.

Previous studies have shown that some miRNAs are abnormally expressed in myocardial tissue and can be involved in physiological processes such as cardiomyocyte apoptosis [43,44]. For example, the study of Luo et al. concluded that the expression of miR-495-3p was significantly depleted in rats with MI/RI, and long noncoding RNA nuclear paraspeckle assembly transcript 1 (LncRNA NEAT1) exacerbated MI/RI by down-regulating miR-495-3p expression [23]; miR-181c-5p exacerbates H/R-induced cardiomyocyte apoptosis via targeting protein tyrosine phosphatase nonreceptor type 4 (PTPN4) [24]. In order to gain further insight into the specific mechanisms involved in the process of MI/RI by TNC, we combined three databases to screen potential upstream miRNAs of TNC, and investigated each of these candidates in the relevant literature. Consistently, we corroborated the target relationship between miR-495-3p and TNC by dual luciferase assay, as well as verified the low expression of miR-495-3p in H9C2 cells after H/R treatment. Besides, the further research revealed that in H/R-induced cells, miR-495-3p depletion remarkably up-regulated the expression of TNC, which was overturned with the addition of TNC silencing. Thus, we speculated that miR-495-3p could engage in the apoptosis and inflammation of cardiomyocytes during MI/RI by targeting TNC. The current results of rescue experiments demonstrated that miR-495-3p depletion reversed the protecting effect of TNC silencing on H/R-induced H9C2 cells by increasing apoptosis and reducing

viability. It has been reported that miRs show a close relation with cell injury and Ca2+ overload during MI/RI, miR-214 protects the mouse heart from ischemic injury by controlling Ca^{2+} overload and cell death [45]; in addition, dexmedetomidine alleviates MI/RI and Ca^{2+} overload via the miR-346-3p/CaMKIId axis [42]. In this study, we found that inhibition of miR-495-3p increased Ca^{2+}, TNF-α and IL-1β levels and decreased MMP level and it reversed the effect of TNC silencing on the H/R-induced H9C2 cells.

5. Conclusions

In conclusion, our study unveiled that miR-495-3p depletion targeting TNC facilitated the injury of H/R-induced cardiomyocytes through promoting apoptosis and inflammation, which might be mediated by Ca^{2+} overload-driven mitochondrial dysfunction. Furthermore, it is revealed that miR-495-3p could serve as a potential marker to monitor the progression of MI/RI, and TNC may be a novel target gene for alternative cardioprotective strategies. However, the inadequacy of this study is that the detection of miR-495-3p/TNC axis functioning *in vivo* was not considered, which we will improve in the next stage of study.

Funding

Authors' Contributions

Substantial contributions to conception and design: WS. Data acquisition, data analysis and interpretation: NQ. Drafting the article or critically revising it for important intellectual content: WS. Final approval of the version to be published: All authors. Agreement to be accountable for all aspects of the work in ensuring that questions related to the accuracy or integrity of the work are appropriately investigated and resolved: All authors.

Data availability statement

The analysed data sets generated during the study are available from the corresponding author on reasonable request.

Conflict of interest

The authors declare no conflicts of interest.

Acknowledgements

References

[1] Mozaffarian D, Benjamin EJ, Go AS, Arnett DK, Blaha MJ, Cushman M, et al. Heart disease and stroke statistics–2015 update: a report from the American Heart Association. Circulation 2015;131:e29–322.

[2] Libby P. Mechanisms of acute coronary syndromes and their implications for therapy. N Engl J Med 2013;368:2004–13.

[3] Hausenloy DJ, Yellon DM. Myocardial ischemia-reperfusion injury: a neglected therapeutic target. J Clin Invest 2013;123:92–100.

[4] Powers SK, Murlasits Z, Wu M, Kavazis AN. Ischemia-reperfusion-induced cardiac injury: a brief review. Med Sci Sports Exerc 2007;39:1529–36.

[5] Midwood KS, Chiquet M, Tucker RP, Orend G. Tenascin-C at a glance. J Cell Sci 2016;129:4321–7.

[6] Faissner A, Roll L, Theocharidis U. Tenascin-C in the matrisome of neural stem and progenitor cells. Mol Cell Neurosci 2017;81:22–31.

[7] Chen S, Fu H, Wu S, Zhu W, Liao J, Hong X, et al. Tenascin-C protects against acute kidney injury by recruiting Wnt ligands. Kidney Int 2019;95:62–74.

[8] Gao W, Li J, Ni H, Shi H, Qi Z, Zhu S, et al. A potential biomarker for predicting the severity of coronary atherosclerosis. J Atherosclerosis Thromb 2019;26:31–8.

[9] Wang Z, Wei Q, Han L, Cao K, Lan T, Xu Z, et al. Tenascin-c renders a proangiogenic phenotype in macrophage via annexin II. J Cell Mol Med 2018;22:429–38.

[10] Imanaka-Yoshida K, Aoki H. Tenascin-C and mechanotransduction in the development and diseases of cardiovascular system. Front Physiol 2014;5:283.

[11] Nishioka T, Onishi K, Shimojo N, Nagano Y, Matsusaka H, Ikeuchi M, et al. Tenascin-C may aggravate left ventricular remodeling and function after myocardial infarction in mice. Am J Physiol Heart Circ Physiol 2010;298:H1072–8.

[12] Ballard VL, Sharma A, Duignan I, Holm JM, Chin A, Choi R, et al. Vascular tenascin-C regulates cardiac endothelial phenotype and neovascularization. Faseb J 2006;20:717–9.

[13] Song J, Yu J, Li Y, Lu S, Ma Z, Shi H. MR targeted imaging for the expression of tenascin-C in myocardial infarction in vivo. J Magn Reson Imag : JMRI 2017;45:1668–74.

[14] Gonçalves IF, Acar E, Costantino S, Szabo PL, Hamza O, Tretter EV, et al. Epigenetic modulation of tenascin C in the heart: implications on myocardial ischemia, hypertrophy and metabolism. J Hypertens 2019;37:1861–70.

[15] Jin L, Hastings NE, Blackman BR, Somlyo AV. Mechanical properties of the extracellular matrix alter expression of smooth muscle protein LPP and its partner palladin; relationship to early atherosclerosis and vascular injury. J Muscle Res Cell Motil 2009;30:41–55.

[16] Liu B, Li J, Cairns MJ. Identifying miRNAs, targets and functions. Briefings Bioinf 2014;15:1–19.

[17] Zhou SS, Jin JP, Wang JQ, Zhang ZG, Freedman JH, Zheng Y, et al. miRNAS in cardiovascular diseases: potential biomarkers, therapeutic targets and challenges. Acta Pharmacol Sin 2018;39:1073–84.

[18] Shi J, Bei Y, Kong X, Liu X, Lei Z, Xu T, et al. miR-17-3p contributes to exercise-induced cardiac growth and protects against myocardial ischemia-reperfusion injury. Theranostics 2017;7:664–76.

[19] Ding S, Liu D, Wang L, Wang G, Zhu Y. Inhibiting MicroRNA-29a protects myocardial ischemia-reperfusion injury by targeting SIRT1 and suppressing oxidative stress and NLRP3-mediated pyroptosis pathway. J Pharmacol Exp Therapeut 2020;372:128–35.

[20] Huang ZQ, Xu W, Wu JL, Lu X, Chen XM. MicroRNA-374a protects against myocardial ischemia-reperfusion injury in mice by targeting the MAPK6 pathway. Life Sci 2019;232:116619.

[21] Lin X, Lin Q. MiRNA-495-3p attenuates TNF-α induced apoptosis and inflammation in human nucleus pulposus cells by targeting IL5RA. Inflammation 2020;43:1797–805.

[22] He Y, Sun Y, Peng J. Circ_0114428 regulates sepsis-induced kidney injury by targeting the miR-495-3p/CRBN Axis. Inflammation 2021;44:1464–77.

[23] Luo M, Sun Q, Zhao H, Tao J, Yan D. Long noncoding RNA NEAT1 sponges miR-495-3p to enhance myocardial ischemia-reperfusion injury via MAPK6 activation. J Cell Physiol 2020;235:105–13.

[24] Ge L, Cai Y, Ying F, Liu H, Zhang D, He Y, et al. miR-181c-5p exacerbates hypoxia/reoxygenation-induced cardiomyocyte apoptosis via targeting PTPN4. Oxid Med Cell Longev 2019:1957920.

[25] Livak KJ, Schmittgen TD. Analysis of relative gene expression data using real-time quantitative PCR and the 2(-Delta Delta C(T)) Method. Methods (San Diego, CA, US) 2001;25:402–8.

[26] Turer AT, Hill JA. Pathogenesis of myocardial ischemia-reperfusion injury and rationale for therapy. Am J Cardiol 2010;106:360–8.

[27] Peter ME, Heufelder AE, Hengartner MO. Advances in apoptosis research. Proc Natl Acad Sci USA 1997;94:12736–7.

[28] Gottlieb RA, Burleson KO, Kloner RA, Babior BM, Engler RL. Reperfusion injury induces apoptosis in rabbit cardiomyocytes. J Clin Invest 1994;94:1621–8.

[29] Madonna R, Bolli R, Rokosh G, De Caterina R. Targeting phosphatidylinositol 3-kinase-Akt through hepatocyte growth factor for cardioprotection. J Cardiovasc Med 2013;14:249–53.

[30] Shiroto K, Otani H, Yamamoto F, Huang CK, Maulik N, Das DK. MK2-/- gene knockout mouse hearts carry anti-apoptotic signal and are resistant to ischemia reperfusion injury. J Mol Cell Cardiol 2005;38:93–7.

[31] White MY, Tchen AS, McCarron HC, Hambly BD, Jeremy RW, Cordwell SJ. Proteomics of ischemia and reperfusion injuries in rabbit myocardium with and without intervention by an oxygen-free radical scavenger. Proteomics 2006;6:6221–33.

[32] Sanada S, Komuro I, Kitakaze M. Pathophysiology of myocardial reperfusion injury: preconditioning, postconditioning, and translational aspects of protective measures. Am J Physiol Heart Circ Physiol 2011;301:H1723–41.

[33] Wang X, Guo Z, Ding Z, Mehta JL. Inflammation, autophagy, and apoptosis after myocardial infarction. J Am Heart Assoc 2018;7.

[34] Deng X, Yang P, Gao T, Liu M, Li X. Allicin attenuates myocardial apoptosis, inflammation and mitochondrial injury during hypoxia-reoxygenation: an in vitro study. BMC Cardiovasc Disord 2021;21:200.

[35] Zhou CN, Yao W, Gong YN, Li Y, Wang CH, Huo YF. 22-oxacalcitriol protects myocardial ischemia-reperfusion injury by suppressing NF-κB/TNF-α pathway. Eur Rev Med Pharmacol Sci 2019;23:5495–502.

[36] Yuan X, Xiang Y, Zhu N, Zhao X, Ye S, Zhong P, et al. Salvianolic acid A protects against myocardial ischemia/reperfusion injury by reducing platelet activation and inflammation. Exp Ther Med 2017;14:961–6.

[37] Tong X, Zhang J, Shen M, Zhang J. Silencing of tenascin-C inhibited inflammation and apoptosis via PI3K/akt/NF-κB signaling pathway in subarachnoid hemorrhage cell model. J Stroke Cerebrovasc Dis 2020;29:104485.

[38] Tajiri K, Yonebayashi S, Li S, Ieda M. Immunomodulatory role of tenascin-C in myocarditis and inflammatory cardiomyopathy. Front Immunol 2021;12: 624703.

[39] Zhou H, Zhang Y, Hu S, Shi C, Zhu P, Ma Q, et al. Melatonin protects cardiac microvasculature against ischemia/reperfusion injury via suppression of mitochondrial fission-VDAC1-HK2-mPTP-mitophagy axis. J Pineal Res 2017;63.

[40] Kagan VE, Borisenko GG, Tyurina YY, Tyurin VA, Jiang J, Potapovich AI, et al. Oxidative lipidomics of apoptosis: redox catalytic interactions of cytochrome c with cardiolipin and phosphatidylserine. Free Radical Biol Med 2004;37: 1963–85.

[41] Yuan M, Meng XW, Ma J, Liu H, Song SY, Chen QC, et al. Dexmedetomidine protects H9c2 cardiomyocytes against oxygen-glucose deprivation/ reoxygenation-induced intracellular calcium overload and apoptosis through regulating FKBP12.6/RyR2 signaling. Drug Des Dev Ther 2019;13: 3137–49.

[42] Zheng X, Li J, Fan Q, Zhao X, Chen K. Dexmedetomidine alleviates myocardial ischemia/reperfusion-induced injury and Ca(2+) overload via the microRNA-346-3p/CaMKIId axis. Int J Cardiol 2021;338:185–95.

[43] Han F, Chen Q, Su J, Zheng A, Chen K, Sun S, et al. MicroRNA-124 regulates cardiomyocyte apoptosis and myocardial infarction through targeting Dhcr24. J Mol Cell Cardiol 2019;132:178–88.

[44] Wojciechowska A, Braniewska A, Kozar-Kamińska K. MicroRNA in cardiovascular biology and disease. Adv Clin Exp Med 2017;26:865–74.

[45] Aurora AB, Mahmoud AI, Luo X, Johnson BA, van Rooij E, Matsuzaki S, et al. MicroRNA-214 protects the mouse heart from ischemic injury by controlling Ca^{2+} overload and cell death. J Clin Invest 2012;122:1222–32.